THE JOURNAL OF BIOLOGICAL CHEMISTRY VOL. 287, NO. 10, pp. 7615–7625, March 2, 2012

Apolipoprotein A-II-mediated Conformational Changes of Apolipoprotein A-I in Discoidal High Density Lipoproteins*[S]

Received for publication, August 7, 2011, and in revised form, January 6, 2012 Published, JBC Papers in Press, January 10, 2012, DOI 10.1074/jbc.M111.291070

Kekulawalage Gauthamadasa[‡], Nataraja Sarma Vaitinadin[‡], James L. Dressman[‡], Stephen Macha[§], Reyn Homan[¶], Kenneth D. Greis[‖], and R. A. Gangani D. Silva[‡1]

From the [‡]Department of Pathology and Laboratory Medicine, Center for Lipids and Atherosclerosis Sciences, and the [‖]Department of Cancer and Cell Biology, University of Cincinnati, Cincinnati, Ohio 45267, the [§]Department of Chemistry, Mass Spectrometry Services, University of Cincinnati, Cincinnati, Ohio 45221, and [¶]AlphaCore Pharma, Ann Arbor, Michigan 48103

Background: Role of apolipoprotein (apo) A-II on metabolism of high density lipoproteins (HDLs) is unknown.
Results: Conformational changes of apoA-I, the major apolipoprotein of HDL, caused by apoA-II in discoidal HDL are confined to two regions of apoA-I.
Conclusion: Interactions between the two major apolipoproteins in discoidal HDL are site specific.
Significance: Functional implications of HDL complexes will significantly benefit from such structural information.

It is well accepted that HDL has the ability to reduce risks for several chronic diseases. To gain insights into the functional properties of HDL, it is critical to understand the HDL structure in detail. To understand interactions between the two major apolipoproteins (apos), apoA-I and apoA-II in HDL, we generated highly defined benchmark discoidal HDL particles. These particles were reconstituted using a physiologically relevant phospholipid, 1-palmitoyl-2-oleoyl-*sn*-glycero-3-phosphocholine (POPC) incorporating two molecules of apoA-I and one homodimer of apoA-II per particle. We utilized two independent mass spectrometry techniques to study these particles. The techniques are both sensitive to protein conformation and interactions and are namely: 1) hydrogen deuterium exchange combined with mass spectrometry and 2) partial acetylation of lysine residues combined with MS. Comparison of mixed particles with apoA-I only particles of similar diameter revealed that the changes in apoA-I conformation in the presence of apoA-II are confined to apoA-I helices 3–4 and 7–9. We discuss these findings with respect to the relative reactivity of these two particle types toward a major plasma enzyme, lecithin:cholesterol acyltransferase responsible for the HDL maturation process.

Due to several beneficial properties of high density lipoproteins (HDLs),[2] it is currently considered a major therapeutic target. In addition to well known anti-atherogenic properties (1–3), other known beneficial roles of HDL include host defense, platelet aggregation, and vasodilation (2, 4–7). Apolipoproteins of HDL are thought to play a major role in the beneficial functions of HDL. Although recent mass spectrometry identifications reported HDL to contain up to 70 different proteins (8, 9), ~90% of HDL protein content is made up of two major apolipoproteins (apos), apoA-I and apoA-II. The average molar ratio of apoA-I:apoA-II in HDL is reported to be 2:1 (10, 11).

The presence of apoA-II divides HDL into two subpopulations based on apolipoprotein composition: HDL that contains both apoA-I and apoA-II (LpA-I/A-II), and HDL that contains apoA-I but not apoA-II (LpA-I). Both LpA-I and LpA-I/A-II are reported to be heterogenous within themselves based on their protein stoichiometry (12, 13). The reported evidence suggests that LpA-I/A-II is the predominant HDL subpopulation (12, 14).

Highlighting the importance of apoA-II, several clinical trials have reported that apoA-II is a negative risk factor for cardiovascular disease as seen for apoA-I (15–17). However, the majority of studies on apoA-II implementing murine models have contradicted these outcomes possibly due to interspecies differences (18–21). For example, human apoA-II[3] is a 17.4-kDa homodimer consisting of two 77-residue monomer strands, linked via Cys residues at position 6 (18, 22). Murine apoA-II lacks Cys and hence exists as a monomer. Moreover, murine apoA-II shares only 60% sequence homology with human apoA-II.

Despite the predominance of the LpA-I/A-II subpopulation, relatively little work has been performed to understand apoA-I-apoA-II interactions in HDL. A study performed on mixed

* This work was supported, in whole or in part, by National Institutes of Health Grant K99/R00 HL087561 (to R. A. G. D. S.) from the NHLBI and a grant from the University of Cincinnati Millennium Scholars' fund (to K. D. G.).

[S] This article contains supplemental Tables S1 and S2, Fig. S1, and "Experimental Procedures."

[1] To whom correspondence should be addressed: 2120 Galbraith Rd., Cincinnati, OH 45237-0507. Tel.: 513-558-4325; Fax: 513-558-1312; E-mail: silvar@ucmail.uc.edu.

[2] The abbreviations used are: HDL, high density lipoprotein; Ac_2O, acetic anhydride; A-I dHDL, reconstituted discoidal HDL particles that contain only apoA-I; A-I/A-II dHDL, reconstituted discoidal HDL that contain both apoA-I and apoA-II; apo, apolipoprotein; BS^3, bis(sulfosuccinimidyl)suberate; CE, cholesteryl ester; DPPC, 1,2-dipalmitoyl-*sn*-glycero-3-phosphocholine; FC, free cholesterol; LCAT, lecithin:cholesterol acyltransferase; LpA-I, human HDL particles that mainly contain apoA-I but not apoA-II; LpA-I/A-II, human HDL particles that contain both apoA-I and apoA-II; MS/MS, tandem mass spectrometry; POPC, 1-palmitoyl-2-oleoyl-*sn*-glycero-3-phosphatidylcholine; SEC, size exclusion chromatography; dHDL, discoidal HDL; HDX-MS, hydrogen deuterium exchange-mass spectrometry.

[3] Human apoA-II is most commonly found in circulation as a disulfide-linked homodimer of 77 amino acid apoA-II monomer strands. For the purposes of this article, we use the term apoA-II molecule to refer to this apoA-II homodimer.

discoidal HDL (dHDL) reported that four putative helices of apoA-I spanning residues 99–187 (helices 4–7) form a hinge domain in the presence of apoA-II (11). This was reported based on outcomes from a limited proteolysis experiment, which resulted in a unique 14-kDa apoA-I fragment from mixed particles. Another study, focused on spherical particles with the use of epitope mapping, suggested that the central region of apoA-I (residues 98–186 spanning helices 4–7) is relatively buried in LpA-I/A-II particles compared with these residues in LpA-I. The study reported that the structural changes of apoA-I occurs more toward the N and C termini in the presence of apoA-II (23). Rye *et al.* (24) reported a decrease in monoclonal antibody binding to three epitopes in the C-terminal domain of apoA-I in mixed spherical particles. However, these techniques could not pinpoint specific protein interactions, and the locations of the conformational changes in the apoA-I sequence in the presence of apoA-II.

In the current study, we report apoA-I-apoA-II interactions in highly defined discoidal HDL particles. In this regard, we utilized two independent state of the art mass spectrometry (MS) techniques that are sensitive to structural details: hydrogen deuterium exchange combined with mass spectrometry (HDX-MS), and partial acetylation of Lys residues combined with MS. Based on our findings, we report that apoA-I-apoA-II interactions in discoidal HDL are confined to two apoA-I regions, putative helices 3–4 and 7–9. Furthermore, we discuss the effect of apoA-II on LCAT activity of these particles, a critical plasma factor responsible in HDL maturation.

EXPERIMENTAL PROCEDURES

Apolipoprotein Purification and Reconstitution of dHDL Particles—ApoA-I and apoA-II isolation and purification from fresh-pooled human plasma was carried out as reported before (11, 25). In brief, total HDL was isolated by ultracentrifugation. Upon delipidation, apoA-I and apoA-II were separated on a Q-Sepharose fast flow anion exchange column. The isolated apolipoproteins were subjected to a final purification on a Superdex 200 size exclusion chromatography column (SEC, GE Healthcare) just prior to particle reconstitution. The SEC fractions containing only dimeric apoA-II were used in particle reconstitution.

Discoidal HDL containing only apoA-I (termed A-I dHDL) was prepared using the Bio-Bead/cholate removal method as reported before (26, 27). An initial molar ratio of 1:78 apoA-I: 1-palmitoyl-2-oleoyl-*sn*-glycero-3-phosphocholine (POPC, Avanti Polar Lipids, Birmingham, AL) was used. Once prepared, A-I dHDL particles were repurified using a tandem SEC setup (Superdex 200 and Superose 6, GE Healthcare) to remove any lipids and proteins not bound to the particles. For apoA-I and apoA-II mixed discoidal HDL (A-I/A-II dHDL) reconstitution, repurified A-I dHDL was incubated at 37 °C for 48 h at a protein concentration of 0.1 mg/ml in 20 mM phosphate-buffered saline (PBS) to fully equilibrate various conformational subpopulations of A-I dHDL. Next, apoA-II was introduced at a molar ratio of 200:95 apoA-I:apoA-II, and the solution was incubated at 4 °C for an additional 48 h. This ratio has been reported to generate mixed apoA-I and apoA-II particles without displacing any apoA-I from 1,2-dipalmitoyl-*sn*-glycero-3-phosphocholine (DPPC) particles (11). SEC analysis carried out upon apoA-II introduction into A-I dHDL confirmed that there was no detectable displaced apoA-I from the particles. Hence A-I/A-II dHDL particles were used in the study without a SEC purification step. The A-I/A-II dHDL were concentrated by ultrafiltration to 1 mg/ml of total protein and then used for analysis within 3 days. The final composition of A-I dHDL and A-I/A-II dHDL are reported in Table 1.

Western Blot Analysis—A-I dHDL, A-I/A-II dHDL, and free proteins (4 μg of protein/lane) were subjected to native PAGE on a 8–25% native Phast gel and transferred to a nitrocellulose membrane. ApoA-I was detected using a primary rabbit antibody (dilution 1:3500, catalog number 178422, Calbiochem, San Diego, CA) and secondary anti-rabbit antibody (dilution 1:20,000, catalog number NA934V, GE Healthcare). ApoA-II was detected with primary goat antibody (dilution 1:3500, catalog number 178464, Calbiochem, San Diego, CA) and a secondary anti-goat antibody (dilution 1:20,000, catalog number 605-703-002, Rockland, Gilbertsville, PA). The total protein concentration was determined by modified Markwell Lowry protein assay (28).

MALDI-MS—Mass spectrometry measurements were carried out using methods developed in our laboratory as reported before (12, 29). Briefly, the cross-linker, bis(sulfosuccinimidyl-)suberate (BS^3, Pierce), was added to dHDL particles at a total protein to cross-linker molar ratio of 1:100 and the solution was incubated for 24 h. Upon delipidation, samples were subjected to mass spectrometry measurements on a Bruker Daltonics MALDI-TOF mass spectrometer (Billerica, MA) (12, 29).

HDX-MS Measurements—Deuterium incorporation into the amide backbone of apoA-I in A-I dHDL and A-I/A-II dHDL as a function of time was monitored using three independent A-I dHDL and A-I/A-II dHDL particle preparations. The experiments were carried out adapting the methods reported before as required for the mass spectrometry system available to us (QStar-XL, AB Sciex, Foster City, CA). The detailed methodology for the experimental approach is given under supplemental "Experimental Procedures" (30–32).

Apolipoprotein Lys Modification by Acetic Anhydride and Processing for MS—Differences in surface exposure of Lys residues on apoA-I incorporated in A-I dHDL and A-I/A-II dHDL were monitored, subjecting three independent particle preparations to acetic anhydride (Ac_2O) modifications. The methodology details are given under supplemental "Experimental Procedures."

Proteolytic Digestion—Limited tryptic digestion experiments on A-I dHDL and A-I/A-II dHDL were carried out using similar experimental conditions as reported before (11). Two sets of independently prepared particles were subjected to proteolysis.

Lecithin:Cholesterol Acyltransferase (LCAT) Assay—A-I dHDL and A-I/A-II dHDL particles for LCAT assay were prepared as described above, except that in addition to apoA-I and POPC, these particles contained a small amount of free cholesterol (FC). For A-I dHDL the starting proportion of POPC:FC: apoA-I was 80:5:1. From the total amount of FC, about 10% of FC consisted of tritiated [^{3}H]cholesterol (PerkinElmer Life Sciences). The amounts of [^{3}H]cholesterol were chosen for the final particles used in the assay (0.5 mg/ml, 20 μl sample vol-

ume) to result in 5000 cpm. The particle diameters, based on native PAGE, were identical to the particles used in HDX-MS and Ac_2O modification experiments (data not shown). The assay was performed as reported before (11, 33). Upon LCAT reaction, the entire lipid content was extracted and separated using thin layer chromatography (TLC) using a solvent system containing petroleum ether:ethyl ether:acetic acid (85:15:1). Separated FC and cholesteryl ester (CE) bands were scraped from TLC plates and the amounts of [^{3}H]cholesterol in each band were determined by scintillation counting.

Statistical Analysis—Statistical analyses were performed on data collected from three independent particle preparations using a two-tailed equal variance *t* test. Statistical comparisons were made between the sets of similar apoA-I peptides generated from A-I dHDL and A-I/A-II dHDL. There are no statistical corrections on the data sets for multiple peptide comparisons.

RESULTS

Characterization of A-I/A-II dHDL Particles—To understand the interactions between apoA-I and apoA-II, we reconstituted a stable A-I/A-II dHDL particle with a highly defined composition. Durbin and Jonas (11) had previously reported a method for mixed discoidal HDL generation, in which varying amounts of apoA-II were introduced into a medium containing preformed apoA-I only discoidal HDL. They reported that apoA-II could displace apoA-I from discoidal HDL when apoA-II exceeds the 2:1 apoA-I:apoA-II ratio, but not below. Based on the average protein ratios used, the particles were reported to contain two molecules of apoA-I and one molecule apoA-II. We began by applying this method to produce stable mixed particles. However, we chose to use POPC as the lipid, rather than DPPC, as it is more representative of the fluid mixed chain lipids found in plasma HDL. During our initial attempts, we used 1 mg/ml of particle concentration and a 20-min incubation step upon apoA-II introduction, as was reported before (11). These conditions generated particles that appeared homogeneous by native PAGE, but were found to be heterogeneous in terms of apolipoprotein stoichiometry per particle upon particle cross-linking followed by SDS-PAGE analysis (data not shown). Given that particles prepared with only apoA-I and only apoA-II generate particles with almost identical hydrodynamic diameters (26, 34, 35), it is perhaps not surprising that heterogeneous mixed protein compositions also generate similar diameter particles. Upon further experimentation, we found that it was necessary to incubate the parent A-I dHDL particles for 48 h at 37 °C prior to the introduction of apoA-II. Moreover, the incubation must be carried out at a low particle concentration of 0.1 mg/ml, because incubations at high concentrations resulted in the change of particle diameter with generation of heterogeneous particle populations as seen by native PAGE (data not shown). Upon apoA-II introduction, particles were incubated for another 48 h. A-I/A-II dHDL particles were generated using our optimized method, exhibited a comparable Stokes diameter to the parental A-I dHDL particles, as seen by native PAGE (Fig. 1*A* and Table 1). Fig. 1*B* shows an SDS-PAGE analysis of the same particles in Fig. 1*A*, demonstrating their protein composition. At first glance, the Coomassie staining suggests less apoA-II in the particles than 2:1 apoA-I:apoA-II. This is due to apoA-II having a lower capacity to bind with the staining dye compared with apoA-I. Different Coomassie staining capacities of apoA-I and apoA-II are demonstrated in supplemental Fig. S1.

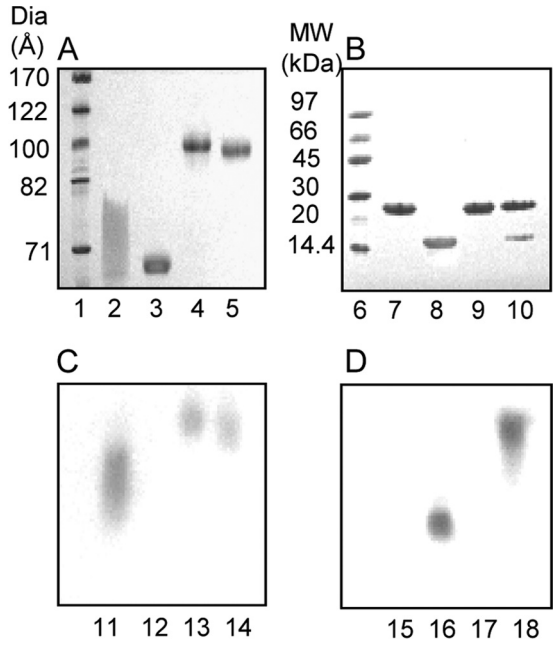

FIGURE 1. **PAGE and Western blot characterization of dHDL particles used in the study.** *A,* native PAGE (8–25% Phast gel, GE Healthcare) of A-I dHDL (*lane 4*) and A-I/A-II dHDL (*lane 5*). *B,* SDS-PAGE (8–25%, Phast gel, GE Healthcare) of A-I dHDL (*lane 9*) and A-I/A-II dHDL (*lane 10*) under nonreducing conditions. Free apoA-I, *lanes 2* and *7*. Free apoA-II, *lanes 3* and *8*. GE Healthcare high and low molecular weight standards are shown in *lanes 1* and *6*, respectively. The gels were stained with Coomassie Blue. *C* and *D,* Western blot analyses of dHDL particles with anti-apoA-I and anti-apoA-II antibodies, respectively. A-I dHDL, *lanes 13* and *17*; A-I/A-II dHDL, *lanes 14* and *18*; free apoA-I, *lanes 11* and *15*; free apoA-II, *lanes 12* and *16*. Western blots were derived from an identical 8–25% Phast gel to the native PAGE in *panel A*.

Next, we confirmed that the incorporation of apoA-II onto A-I dHDL using our optimized method did not displace apoA-I from the particles. For this purpose, we used a variety of approaches including FPLC (see "Experimental Procedures"), native PAGE, and Western blot analyses. Native PAGE did not show any dislodged apoA-I in A-I/A-II dHDL solution (Fig. 1*A*, *lane 5*), which would have migrated similar to free apoA-I (Fig. 1*A*, *lane 2*, note that free apoA-I migrates as a broad band on native gels (24), due to the presence of multiple conformational states). Similar outcomes were observed by Western blot analysis of A-I/A-II dHDL (Fig. 1*C*, *lane 14*). Western blot analysis of the same gel using apoA-II antibodies indicated the absence of free apoA-II in the particle solution (Fig. 1*D*, *lane 18*), indicating that the entire amount of added apoA-II was incorporated into the particles. We also confirmed that 48-h incubations did not cause free apoA-II to partially adsorb to the vessel wall, by determining the apoA-II concentration before and after a 48-h incubation time period (data not shown). Based on these observations, we concluded that the average molar ratio of mixed particles should be closer to 2:1 apoA-I:apoA-II, the starting molecular stoichiometry used in the A-I/A-II dHDL generation.

TABLE 1
Characterization of A-I dHDL and A-I/A-II dHDL particles used in the study

Particle	Particle diameter by PAGE[a]	Numer of apoA-I and apoA-II molecules per particle[b]		Composition PC/A-I/A-II[c]
		ApoA-I	ApoA-II	
	Å			
A-I dHDL	101 ± 1	2	0	75/1
A-I/A-II dHDL	101 ± 2	2	1	147/2/1

[a] Particle diameters were calculated from native PAGE of particles with respect to a known set of high M_r standards (GE Healthcare, catalog number 17-0445-01). Three sets of independently generated particles, including the one shown on Fig. 1, were used.
[b] The number of apoA-I molecules in A-I dHDL were determined by particle cross-linking followed by MALDI-MS (Fig. 2*A*). The average molar ratio of apoA-I:apoA-II in A-I/A-II dHDL and the number of apolipoprotein molecules per A-I/A-II dHDL particle were determined as explained under "Experimental Procedures."
[c] Particle compositions were calculated as described under "Experimental Procedures." The composition of A-I dHDL was determined after the repurification process. The composition of A-I/A-II dHDL was determined after apoA-II incorporation into A-I dHDL without any further purification.

Once we confirmed the average protein molar ratio, we attempted to determine protein stoichiometry of individual particles. The particles were treated with the cross-linking agent BS^3 at a molar ratio of 1:100 (total protein: BS^3), and then analyzed by MALDI-MS (Fig. 2). The parent A-I dHDL exhibited two peaks, ~29.9 kDa (Fig. 2*A*, *peak 1*) and ~59.9 kDa (Fig. 2*A*, *peak 2*), originating from cross-linked monomeric and dimeric apoA-I, respectively (29). The mass ~59.9 kDa, the highest molecular weight appearing in the spectrum represents the mass of two apoA-I molecules cross-linked together. Hence, the result confirmed that A-I dHDL contains two apoA-I per particle, as was reported in numerous studies that utilized discoidal HDL particles of similar morphology (26, 36, 37).

A-I/A-II dHDL also demonstrated peaks corresponding to monomeric and dimeric apoA-I (Fig. 2*B*, *peaks 1* and *2*, respectively). This result confirmed mixed particles also having two molecules of apoA-I per particle. In addition, A-I/A-II dHDL exhibited a peak ~69.5 kDa (Fig. 2*B*, *peak 3*). The M_r of this peak is consistent with a mass generated by cross-linking two molecules of apoA-I and one monomeric strand of apoA-II (half of an apoA-II molecule generated by dissociation of the disulfide bond). However, a peak corresponding to the apoA-I-apoA-II heterodimer generated by cross-linking one molecule of apoA-I and one monomeric strand of apoA-II (~37 kDa) is not seen (Fig. 2*B*). The intensity of the ~69.5 kDa peak seen in the MALDI spectrum did not increase upon the introduction of an additional cross-linker up to 1:400 protein:BS^3 ratio (data not shown). This outcome implied that this mass subjected to unusually lower detection by MALDI-MS or apoA-II in AI/A-II dHDL would be in a highly unfavorable orientation for cross-linking. To further dissect out this observation, we subjected cross-linked A-I/A-II dHDL to SDS-PAGE analysis (Fig. 3). The PAGE analysis demonstrated the presence of a clear band corresponding to two molecules of apoA-I and one molecule of apoA-II cross-linked together (~78 kDa). Moreover, the absence of a band corresponding to free apoA-II (Fig. 3, *lane 2*) on PAGE further confirmed almost all apoA-II cross-linking with apoA-I. The absence of free apoA-II was also seen in MALDI-MS (Fig. 2*B*). Taken together, these observations confirmed that mixed particles contain two molecules of apoA-I and one molecule of apoA-II. Furthermore, apoA-II in the particles is in an orientation that could get cross-linked to apoA-I. This indicated the presence of near neighbor interactions between apoA-I and apoA-II. Low intensity of the ~69.5 kDa peak in the MALDI-MS spectrum could be simply due to the nonquantitative nature of MALDI-MS (29), or due to the specific ion suppression of this mass (38, 39). The strong evidence available for the presence of a trimer, but not apoA-I-apoA-II heterodimer (Figs. 2*B* and 3) implied that protein molecules in A-I/A-II dHDL being in an orientation unfavorable for heterodimer formation.

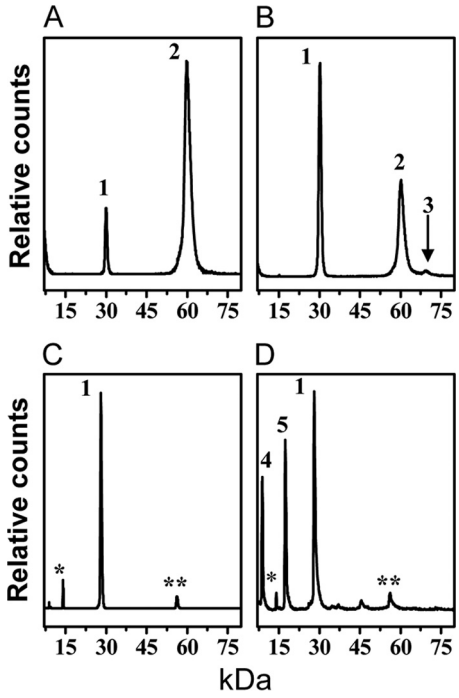

FIGURE 2. **MALDI-MS characterization of A-I dHDL and A-I/A-II dHDL.** *Top panels,* mass spectra of A-I dHDL (*A*) and A-I/A-II dHDL (*B*) cross-linked with BS^3 at a molar ratio of total protein:BS^3, 1:100. The positions of the monomeric A-I (*1*), dimeric A-I (*2*), and the trimer consisting of two molecules of apoA-I and one monomeric stand of apoA-II (*3*), are shown. *Bottom panels,* mass spectra of A-I dHDL (*C*) and A-I/A-II dHDL (*D*) not subjected to cross-linking. The peak positions of monomeric A-I (*1*), single stand of A-II (*4*), and dimeric A-II (*5*) are shown. Minor peaks denoted by *single* (*) and *double* (**) *asterisks* correspond to doubly charged A-I and two associated molecules of A-I baring a single charge, respectively (29).

Structural Information Obtained by HDX-MS—HDX-MS is a reliable method capable of capturing protein conformational changes, and it has been utilized in recent lipoprotein structural studies (30–32). This method has the capability to assess the extent of amide hydrogen involvement in H-bonding together with the extent of their shielding (30). This is done by determining the extent of deuterium incorporation into amide hydrogens in different regions of the protein(s) of interest at selected time intervals. We used HDX-MS to determine variability in deuterium incorporation into different regions of apoA-I in A-I

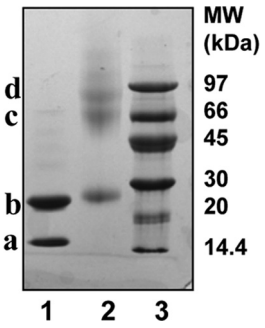

FIGURE 3. **SDS-PAGE characterization of cross-linked A-I/A-II dHDL.** SDS-PAGE (8–25%, Phast gel, GE Healthcare) of A-I/A-II dHDL (*lane 1*), and A-I/A-II dHDL upon cross-linking with 1:100 total protein:BS^3 (*lane 2*). GE Healthcare low molecular weight standards are shown in *lane 3*. *Band a,* ~28 kDa is apoA-I; *band b*, ~60 kDa is two apoA-I molecules cross-linked together; *band c*, ~79 kDa is a trimer consisting of two apoA-I and one apoA-II. The gel was stained with Coomassie Blue.

dHDL *versus* A-I/A-II dHDL. Our goal was to get insights into the conformation and conformational changes of apoA-I in A-I/A-II dHDL with respect to apoA-I in A-I dHDL, in the form of shielding and H-bonding. The experiments were carried out at 7 different preselected time points: 0, 0.5, 1, 5, 15, 180, and 960 min. These specific time points were chosen based on the outcomes from pilot experiments that resulted in the most variation on the extent of deuterium incorporation.

HDX patterns of apoA-I in A-I dHDL showed that there are regions with clearly different conformational properties. To illustrate this, we selected peptic peptides with different deuterium incorporation patterns (Fig. 4). Peptide(148–158), the slowest exchanging peptide of apoA-I, showed only ~80% deuterium incorporation even after 180 min exposure to deuterium. In contrast, peptide(236–243), one of the fastest exchanging peptides, was fully exchanged within the 0.5-min time point. Peptide(1–16) belongs to a region that has moderate rates of deuterium incorporation, and was completely exchanged by the 15-min time point. This data suggested that peptide(236–243) had the least shielding and/or H-bonding, whereas peptide(148–158) had H-bonding and/or shielding to the highest extent.

We identified 39 apoA-I peptic peptides common to all data sets. These peptides span 207 residues that resulted in 85% apoA-I sequence coverage. The list of all peptic peptides and the time taken for them to acquire ≥90% deuterium incorporation are shown in supplemental Table S1. Based on our data, the N-terminal region of apoA-I spanning residues 1–43 demonstrated either fast or moderately fast deuterium incorporation rates. The lipid-bound region spanning helices 1–10 showed variable deuterium incorporation rates that ranged from 0.5 to ≥180 min for completion. Of these, the extreme C terminus (residues 236–243) and residues 45–56 showed the fastest HDX with complete exchange achieved within 0.5 min. Although several of the peptides belonging to helices 1–10 showed fast or moderate deuterium incorporation rates, some peptides belonging to helixes 3–9 showed ≥180 min to achieve complete deuterium exchange, implying that these regions having the highest shielding and/or H-bonding. It is important to note that there is a possibility of two apoA-I molecules in dHDL adapting different conformations. In such a situation HDX data would reflect the average conformation of apoA-I molecules.

Incorporation of apoA-II into dHDL generating A-I/A-II dHDL did not completely change HDX patterns for apoA-I. This observation suggested that apoA-II in A-I/A-II dHDL did not perturb the entire protein backbone of apoA-I. However, two regions of apoA-I exhibited clear differences. These differences are best seen at the 0.5-min time point. Hence, the list of apoA-I peptides identified in both A-I dHDL and A-I/A-II dHDL at the 0.5-min time point, along with % deuterium incorporation, is shown in Fig. 5. As can be seen from the % deuterium incorporation values, the regions of apoA-I that undergo conformational changes in the presence of apoA-II were confined to residues 104–111 (helix 4) and 190–219 (helices 8–9). Importantly, these two regions indicated opposite overall conformational changes. ApoA-I residues 104–111 in A-I/A-II dHDL indicated lower % deuterium incorporation compared with the same residues in A-I dHDL, implying higher shielding and/or H-bonding in this region in the presence of apoA-II. On the other hand, apoA-I residues 190–219 indicated higher % deuterium incorporation when in A-I/A-II dHDL compared with A-I dHDL, implying less shielding and/or H-bonding in the presence of apoA-II. However, as explained above, HDX-MS is not capable of dissecting out the extent of shielding from H-bonding.

Structural Information Obtained by Acetic Anhydride Modification of dHDL Particles—To further dissect out the data generated from HDX-MS, we adapted the Ac_2O approach that has been used on free proteins, and modified it for HDL complexes (40–42). Unlike HDX, which captures a combined effect, partial Ac_2O modifications only determine the extent of shielding of specific sites. This is measured by determining the extent of individual Lys residue modifications by acetylation (40).

During method optimization, we paid particular attention to several important experimental details. First, we optimized the conditions such that there were no unmodified Lys residues at completion of the reaction scheme. This was carried out by utilizing the Mascot Search Engine (Matrix Science) to confirm that there were no detectable proportions of Lys residues that escaped from acetylation. Second, we performed Mascot analysis to confirm that Tyr resides, which are notorious for undergoing acetylation, were not modified by Ac_2O, yielding erroneous interpretations. Third, the initial acetylation step was carried out with extreme caution maintaining physiological pH to sustain native structure of the dHDL (supplemental "Experimental Procedures"). Fourth, we maintained the same molar ratio of Lys:Ac_2O for both types of particles to account for the different numbers of Lys residues in A-I dHDL and A-I/A-II dHDL.

The MS peaks corresponding to apoA-I peptide(180–191) generated from A-I dHDL and A-I/A-II dHDL are shown in Fig. 6. These particles have been subjected to Ac_2O-d_0/Ac_2O-d_6 modifications as explained under "Experimental Procedures." The intensity of the peak resulting from Ac_2O-d_6 modification of apoA-I Lys^{182} in A-I/A-II dHDL is higher (Fig. 6*B*) compared with the corresponding peak in A-I dHDL (Fig. 6*A*). This implies that the extent of the initial modification of Lys^{182} by Ac_2O-d_0 was lower in A-I/A-II dHDL compared with A-I

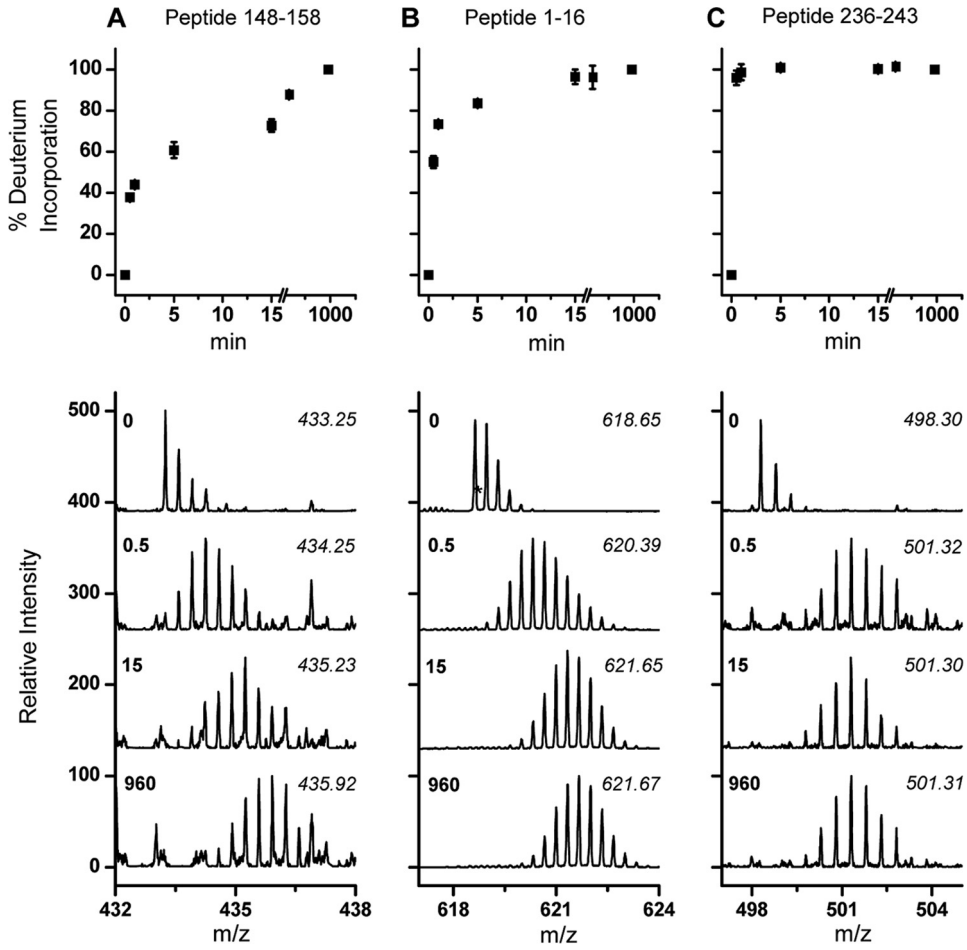

FIGURE 4. **Deuterium incorporation patterns pertinent to different regions of apoA-I in A-I dHDL.** Percent deuterium incorporation into different regions of apoA-I, as a function of time, are listed for three peptic peptides: 148–158 (*A*), 1–16 (*B*), 236–243 (*C*). MS peaks from one representative measurement, at 0-, 0.5-, 15-, and 960-min deuterium incorporation time points, are listed in the *bottom panels*. The *m/z* of the centroid mass of each peak cluster is listed in *italics*. The list of all peptides identified in A-I dHDL and the time taken for complete deuterium incorporation for each of these peptides are listed in supplemental Table S1.

dHDL. In turn, the outcomes imply that the apoA-I Lys^{182} is shielded to a higher extent in A-I/A-II dHDL than in A-I dHDL.

The relative surface exposure of all detected Lys residues of apoA-I in A-I dHDL *versus* A-I/A-II dHDL are shown in Fig. 7. The majority of the apoA-I peptides did not show significant differences in shielding between A-I dHDL and A-I/A-II dHDL. The apoA-I peptides that demonstrated the most differences are confined to two regions of apoA-I spanning helices 3–4 (Lys^{94}, Lys^{96}, Lys^{106}, and Lys^{107}) and helices 7–8 (Lys^{182} and Lys^{195}). Because the Ac_2O technique solely represents the extent of shielding of Lys residues, the data implies that both regions are more shielded in the presence of apoA-II. However, due to lack of Lys residues in apoA-I putative helices 6 and 9, there is no solvent exposure information for these regions. It is important to note that, just as the HDX-MS approach (discussed above), the acetic anhydride modification technique yields average information on individual Lys residues in apoA-I molecules. We were able to detect 19/21 Lys residues in apoA-I upon acetylation, except Lys^{238} and Lys^{239}. The absence of the expected peptides containing these two Lys residues was further confirmed by manually searching the individual spectra.

Limited Proteolysis Experiments—Next, we subjected two independently prepared sets of particles to limited proteolytic experiments using similar proteolytic conditions as reported before (11). Contrary to prior observations, our data on both sets of particles showed identical proteolytic patterns for apoA-I in both A-I dHDL and A-I/A-II dHDL. The outcomes from one experiment are shown in Fig. 8. Our data did not show a unique proteolytic fragment ~14 kDa, generated from A-I/A-II dHDL particles. However, our particles clearly generated the ~22-kDa fragment that was reported in the previous study (11, 43).

LCAT Activity of dHDL Complexes—We also subjected A-I/A-II dHDL and A-I dHDL to LCAT assay (11, 33). LCAT is a plasma enzyme that is critical for the HDL maturation process, which converts FC to CE, which are then stored in the core of HDL. The LCAT activity of these two particle types would yield valuable information as to how the presence of apoA-II would affect LCAT activity of the particle. The protein:LCAT ratio used was determined based on the outcomes from a pilot study performed on the same batch of LCAT used in the experiment, which resulted in 10–50% conversion of FC to CE from A-I dHDL. As illustrated in Fig. 9, A-I/A-II dHDL demonstrated three times lower CE conversion capabilities compared with A-I dHDL (~119 nmol/ml LCAT/h *versus* 322 nmol/ml of LCAT/h, respectively). The outcomes are comparable with the

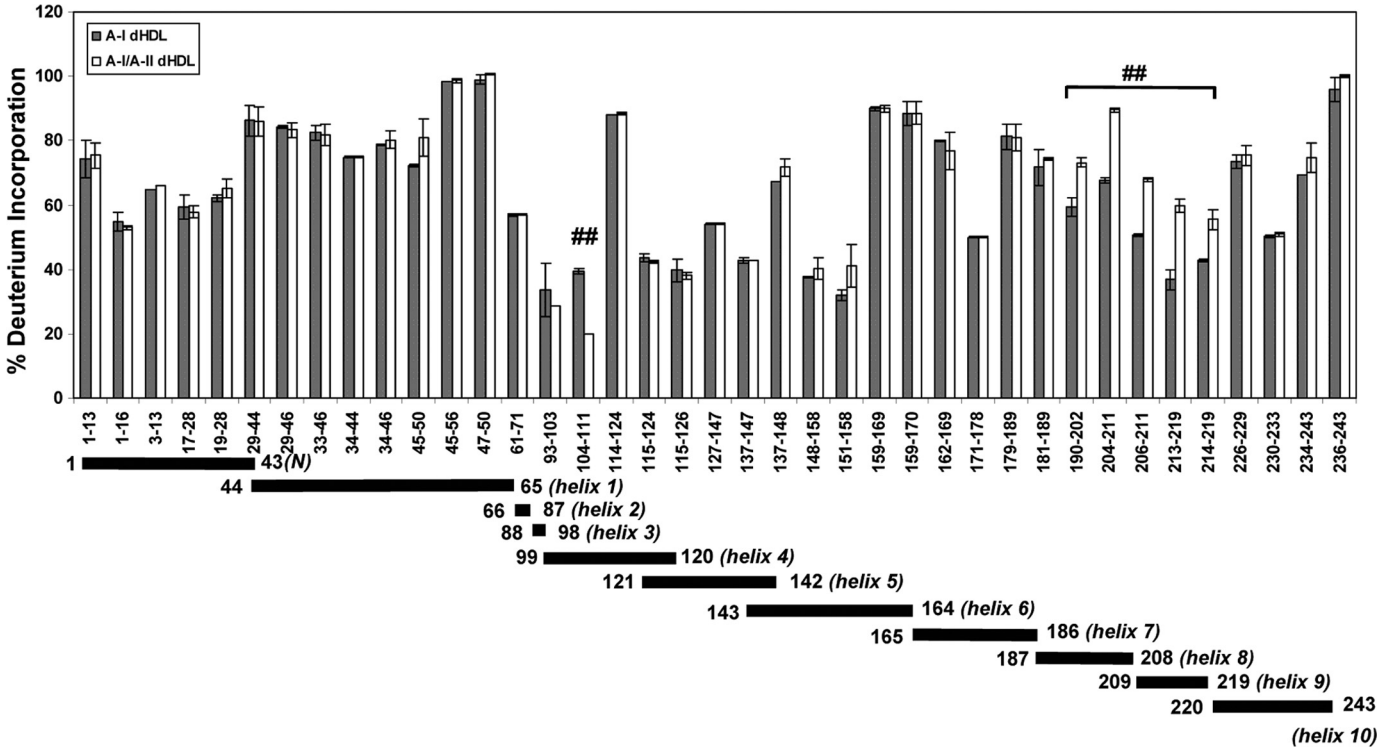

FIGURE 5. **Deuterium incorporation into different regions of apoA-I in A-I dHDL *versus* A-I/A-II dHDL as determined by HDX-MS.** The percent deuterium incorporation into apoA-I in A-I dHDL (*filled bars*) and A-I/A-II dHDL (*open bars*) at the 0.5-min deuterium incorporation time point. Each *bar* represents the average ± S.D. of three experiments performed on three independent particle preparations. ##, $p < 0.01$ for individual apoA-I peptide comparisons between A-I dHDL and A-I/A-II dHDL. Note that there are no statistical corrections for multiple peptide comparisons. The span of identified peptides across apoA-I putative helices is shown *below* the bar graph.

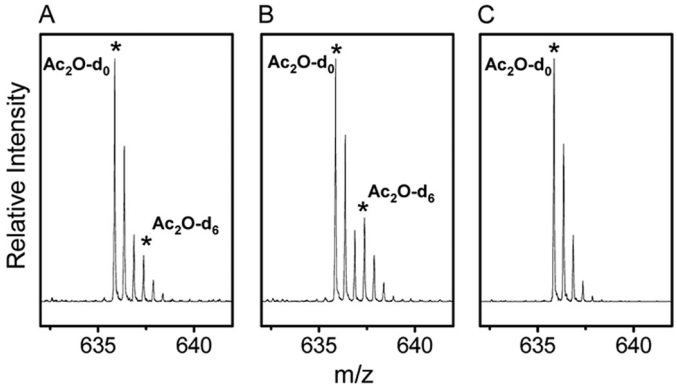

FIGURE 6. **The extent of acetic anhydride modification of apoA-I Lys^{182} in dHDL particles.** Mass spectra of variably modified Lys^{182} in apoA-I, as detected by apoA-I peptide(180–191) (ALKENGGARLAE). *A,* A-I dHDL; *B,* A-I/A-II dHDL. The experimental conditions used for acetylation using Ac_2O-d_0 and Ac_2O-d_6 are explained under "Experimental Procedures." The monoisotopic peaks of the peptide resulted by Ac_2O-d_0 and Ac_2O-d_6 modifications are presented by *asterisks*. The isotopic peak pattern of fully modified peptide in A-I dHDL by Ac2O-d_0 is shown for comparison (*C*).

data reported before for mixed discoidal HDL (11, 43). This outcome clearly demonstrates an inhibitory action of apoA-II on LCAT activity for the mixed particles generated by our optimized method as well.

DISCUSSION

The principal findings of this work are as follows: 1) apoA-I in A-I dHDL showed distinctly different regions with respect to solvent exposure and H-bonded secondary structure; 2) incorporation of apoA-II into A-I dHDL generating A-I/A-II dHDL, had moderate perturbations in the apoA-I structure. The conformational changes caused by apoA-II in apoA-I are confined to two distinct regions spanning apoA-I putative helices 3–4 and 7–9; 3) the limited tryptic digestion demonstrated that both particle types generated identical proteolytic patterns, implying comparable overall conformation for apoA-I in both particles. 4) LCAT activity of mixed particles was lower than A-I dHDL. We discuss our findings below in detail and suggest a model for A-I/A-II dHDL based on these findings.

A-I dHDL—A prior study compared solvent accessibility of apoA-I in dHDL to lipid-free apoA-I using a single 40-s deuterium incorporation time point (31). Based on the extent of deuterium incorporation, the authors concluded that most of apoA-I in dHDL is highly shielded compared with lipid-free apoA-I, except residues 159–180. Our data on deuterium incorporation into different regions of apoA-I in A-I dHDL at 0.5 min are comparable with the reported data (31). Multiple deuterium incorporation time points in our experiment provided additional information on the extent of shielding and H-bonding of apoA-I at different segments.

Our HDX data demonstrated that the N terminus and extreme C terminus of apoA-I exchanged fast or moderately fast compared with the rest of the apoA-I putative helices (supplemental Table S1). Although different peptides in these regions demonstrated somewhat varying deuterium incorporation rates, the extreme C terminus (residues 236–243) demonstrated one of the fastest exchanging capabilities. This outcome implied that the region is highly unstructured and/or solvent exposed. This behavior could be due to the extreme C terminus

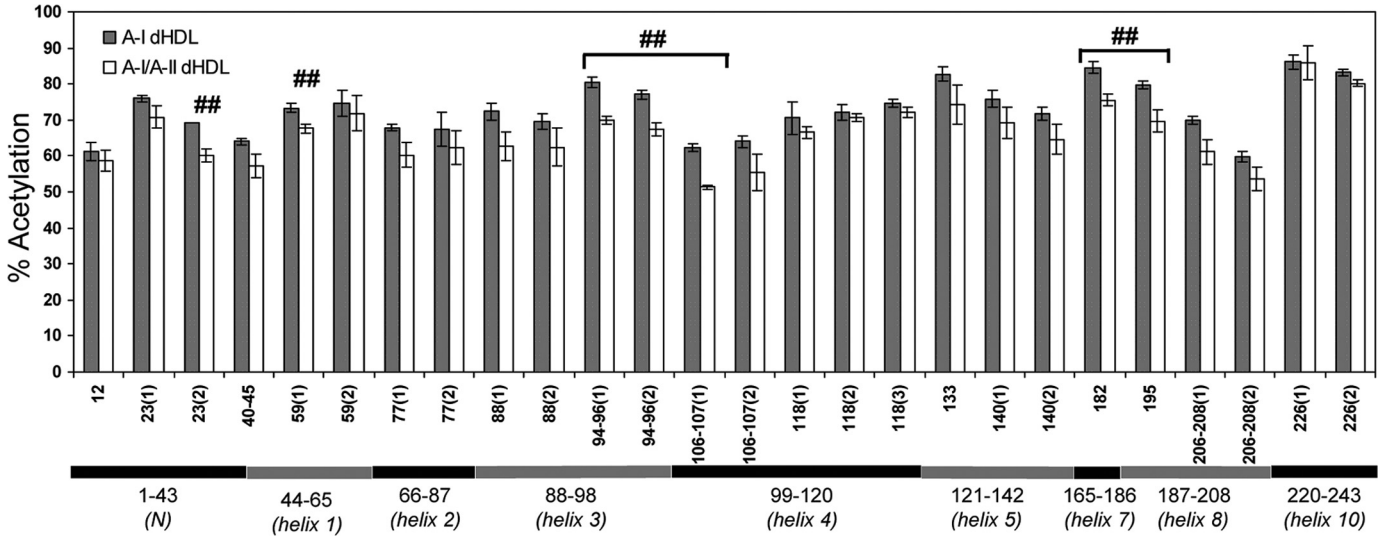

FIGURE 7. **The differences in the surface exposure of Lys residues in A-I dHDL *versus* A-I/A-II dHDL.** The extent of acetylation of apoA-I Lys residues in A-I dHDL and A-I/A-II dHDL were assessed upon Ac_2O-d_0/Ac_2O-d_6 acetylations at pH 7.4 ("Experimental Procedures"). The data presented are the averages of three experiments performed on three independent particle preparations. Each *bar* represents the average ± S.D. for individual peptides. ##, $p < 0.01$ for the individual apoA-I peptides derived from A-I/A-II dHDL *versus* A-I dHDL. Note that statistical corrections were not made for multiple peptide comparisons. Details of all identified peptides are given in supplemental Table S2. Different peptides that contain the same Lys residues are presented as *separate bars*. The mass peaks originating from the same peptide, but with different charge states were averaged. Putative helix distribution is shown *below* the bar graph. Putative helices 6 (143–164) and helix 9 (209–219) do not contain any Lys residues.

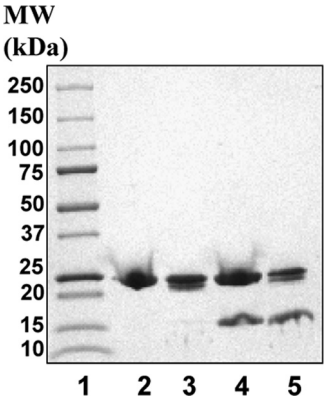

FIGURE 8. **Proteolytic patterns of A-I dHDL and A-I/A-II dHDL.** Particles were subjected to limited proteolytic digestions under similar conditions as reported before (11). Digestions were carried out at 1:200 total protein to trypsin ratio at 37 °C for 2 h. Digestion was quenched by the addition of SDS sample loading buffer followed by boiling for 3 min. Reaction mixtures were analyzed on a 8–25% SDS-Phast gel. *Lane 2*, A-I dHDL; *lane 3*, A-I dHDL subjected to proteolysis; *lane 4*, A-I/A-II dHDL; *lane 5*, A-I/A-II dHDL subjected to proteolysis. Molecular mass markers (Bio-Rad) are on *lane 1*.

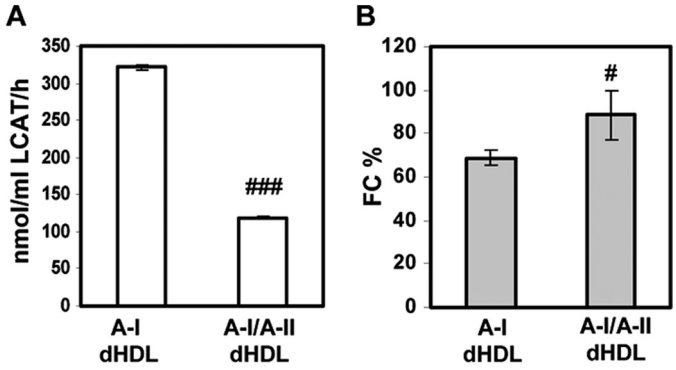

FIGURE 9. **LCAT-mediated cholesteryl ester formation in dHDL particles.** *A*, the rate of cholesteryl ester formation in A-I dHDL and A-I/A-II dHDL were measured as reported before, by subjecting particles to LCAT activity assay (11, 33). *B*, the remaining FC in each particle after the LCAT reaction was estimated as a percentage of initial FC in the particles. *Bars* represent average ± S.D. of three independent experiments. #, $p < 0.05$; ###, $p < 0.001$ between two types of particles.

interacting with highly mobile N terminus (26, 31), which resulted in a highly solvent exposed and unwound C terminus. Highly mobile C terminus is also in agreement with prior molecular modeling studies performed using energy minimizations on lipid-bound apoA-I (31).

Prior studies performed on apoA-I only discoidal HDL, using a fluorescence quenching approach, suggested a hinge domain for 78 Å, apoA-I dHDL, spanning putative helices 5–7 (27). Later experiments carried out using an electron spin resonance technique reported that this hinge region is confined to apoA-I residues 133–146 for ~94 Å apoA-I dHDL (37). One can expect relatively fast deuterium incorporation into a hinge domain, assuming both disrupted amide H-bonding and high solvent exposure that would accompany dislodged segments of apoA-I from the lipid disc edge. However, our data did not show specifically fast deuterium incorporation into this region, and hence does not provide evidence for the presence of a highly unstructured and/or solvent-exposed region (supplemental Table S1). In addition, limited proteolysis experiments did not show the presence of a particularly susceptible site to proteolysis in helices 5–7 supporting HDX-MS findings (Fig. 8).

A-I/A-II Mixed Discoidal HDL—The data generated using both approaches, HDX and Ac_2O, implied that the overall structural changes of apoA-I caused by apoA-II in dHDL are moderate. These findings were further supported by HDX-MS data collected on full-length undigested apoA-I in dHDL particles. At the 0.5-min deuterium incorporation time point, the average mass of apoA-I (28,078 Da) in A-I dHDL increased to 28,159 Da, whereas for A-I/A-II dHDL, the mass increased to 28,161 Da (data not shown). This finding suggested that the overall solvent exposure and secondary structure of apoA-I in

two types of particles are comparable. The moderate perturbing nature of apoA-II on apoA-I in dHDL was also supported, indirectly, by MALDI-MS outcomes (Fig. 2, *A* and *B*). The peak originating from cross-linked dimeric apoA-I in A-I dHDL and A-I/A-II dHDL showed comparable mass shifts upon cross-linking (3,760 and 3,940 Da, respectively). These mass shifts are representative of the average addition of 27 and 28 BS^3 cross-links, respectively (29). Hence, the outcome suggested an overall preservation of "double-belt" architecture for apoA-I in mixed particles, as for apoA-I in A-I dHDL (36, 37, 44, 45).

Both approaches, Ac_2O and HDX-MS, agreed on the regions of apoA-I that underwent conformational changes in both types of particles. One region of apoA-I that demonstrated conformational changes is located in putative helices 3–4 (Figs. 5 and 7). Ac_2O modifications, a direct measure of shielding, implied that Lys residues 94, 96, 106, and 107 are better shielded in mixed particles. HDX-MS detections implied that in A-I/A-II dHDL, the apoA-I segment spanning residues 104–111 is more shielded from the solvent and/or it had undergone additional formation of H-bonding. Combining data from both approaches, we can reliably suggest that putative helices 3–4 of apoA-I in A-I/A-II dHDL are better shielded and have maintained comparable H-bonding compared with the same region of apoA-I in A-I dHDL.

The second region that demonstrated a conformational change is located in apoA-I putative helices 7–9. As for the other region, outcomes from Ac_2O modifications demonstrated higher shielding of apoA-I Lys^{182} and Lys^{195} in A-I/A-II dHDL compared with A-I dHDL. The net combined outcome of HDX implied higher solvent exposure and/or considerable disruption of H-bonding of apoA-I residues 190–219 in the presence of apoA-II. Combining outcomes from both approaches lead to the conclusion that, whereas helices 7–9 in mixed particles are more shielded compared with apoA-I in apoA-I dHDL, the mixed particles have undergone considerably disrupted H-bonds to show higher net deuterium incorporations.

As mentioned above, the previous study on apoA-I and apoA-II mixed dHDL with DPPC reported a hinge domain for apoA-I spanning helices 4–7 (11). This was suggested based on a unique proteolytic site present only in mixed particles that generated a proteolytic fragment of ~14 kDa. Our data on A-I dHDL and A-I/A-II dHDL did not show any detectable conformational changes in helices 4–7. Moreover, the proteolytic experiments performed under similar conditions as before did not show the presence of a unique fragment in A-I/A-II dHDL (Fig. 8). The apparent discrepancy between current data and previous findings could be attributed to different lipids, reconstitution method, and the conformation detection method. One explanation may lie in the extent to which the particles were equilibrated before and after introduction of apoA-II. In our work, a great effort was rendered to develop conditions that resulted in homogeneous particles with the same molecular stoichiometry in individual particles. We suggest that particles formed under these conditions may have allowed both apoA-I and apoA-II to fully equilibrate among the particles, allowing them all to find enough time to acquire the most stable conformation. However, under nonequilibrated conditions in which particle stoichiometry may vary among particles within a preparation, it is likely that apoA-II can exert significant effects on apoA-I conformation.

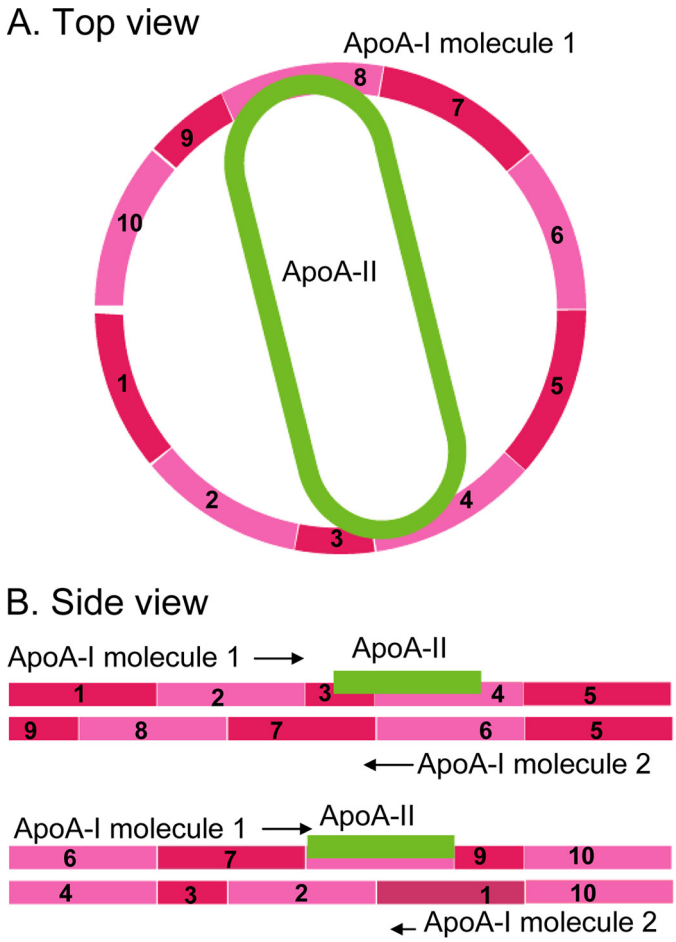

FIGURE 10. **A schematic illustration of apoA-I and apoA-II interactions in reconstituted discoidal HDL.** *A,* top view. The location of apoA-II in the disc, and its interaction sites with apoA-I. *B,* side view. Molecular registry of two apoA-I molecules in the disc using previously published double-belt model as a template (26, 48). Location of the apoA-II with respect to both apoA-I molecules in the disc is shown. Putative helices of apoA-I (*pink*) are numbered. N terminus region of apoA-I (1–43) is not shown. ApoA-II is shown in *green*.

Model—A schematic illustration representing intermolecular contacts between apoA-I and apoA-II in A-I/A-II dHDL is shown in Fig. 10. We used the currently accepted double-belt model for apoA-I discoidal HDL as a template for presenting sites of apoA-I and apoA-II interactions. In this model, apoA-I molecules form amphipathic helical rings in an antiparallel orientation. When stacked on top of each other, these rings encapsulate a circular patch of phospholipid bilayer, protecting fatty acyl chains from aqueous solvent. We started building the model for A-I/A-II dHDL by enforcing the requirement that double-belt architecture is readily preserved in mixed particles (discussed above). Next, we used stoichiometry proportions, *i.e.* the presence of one apoA-II molecule with two apoA-I molecules per particle. Finally, we took into account the resultant data from HDX-MS and Ac_2O approaches and the location of conformational changes of apoA-I in the presence of apoA-II. We enforced these requirements in conjunction with the lipo-

philic nature of apoA-II, by placing the single apoA-II on the face of the disc, mostly buried in the lipids. The same arrangement of apoA-II would fit with the recently proposed alternative to the double-belt model, called the double superhelix model (46), which was reported to maintain most intermolecular contacts proposed by cross-linking studies (26, 36, 45). The only difference would be, however, in the double superhelix model, apoA-II will not be confined to a single phase of the lipid because lipid molecules are encapsulated in a twisted micellar arrangement in this model (46). This low resolution model shows only the regions of apoA-I that have intermolecular contacts with apoA-II. We feel that it is not appropriate to incorporate fine conformational details such as shielding *versus* H-bonding into this model.

At the time of the prior study on dHDL (11) the accepted model for apoA-I in discoidal HDL was the so-called picket fence model (37, 44, 47). In this model apoA-I parallels lipid acyl chains at the bilayer edge as a picket fence with two molecules of apoA-I having the least contact with each other. Since then, numerous studies using independent approaches have generated strong evidence to support the double-belt model (26, 36, 37, 44, 45, 47–49). Hence, we only considered the double-belt model in our discussions above due to the equivocal support for this model from the recent literature.

The current model does not contain any information on apoA-II conformation. To obtain such information using HDX-MS, further method development is necessary to remove all apoA-II-bound lipids, due to the extreme lipophilic nature of apoA-II. Moreover, apoA-I and apoA-II molecular contacts in A-I/A-II dHDL can be obtained by cross-linking approaches followed by LC-MS analyses, as reported for apoA-I only HDL complexes (26, 36, 45). To further test the proposed model, these experiments are currently underway in our laboratory.

LCAT Activity—The central helical regions of apoA-I in discoidal HDL playing a role in LCAT activation have been reported by several laboratories. With the use of apoA-I mutants, it was reported that helices 6–7 (residues 143–186) play an important role in binding LCAT to apoA-I (50). This region was narrowed down to residues 140–150 by Sviridov *et al.* (51). Mixing discoidal apoA-I HDL with LCAT and by monitoring conformational changes with the application of HDX-MS, Wu *et al.* (31) reported that the LCAT interaction site of apoA-I is confined to apoA-I residues 159–170. Assuming that the sites of conformational changes of apoA-I in the presence of apoA-II directly correspond to apoA-I-apoA-II interaction sites, our data suggests that inter-protein interaction sites do not directly overlap with LCAT binding site 159–170 as reported (31). Hence, we propose that apoA-II does not directly interfere with LCAT binding to apoA-I. Rather, the inhibition of LCAT activity by mixed particles could be due to apoA-II acquiring the docking interface of LCAT on the face of the dHDL and competing with LCAT binding. This hypothesis for the current model was also supported by previous findings that reported a reduction in LCAT binding but similar maximum velocities for both apoA-I only and apoA-I and apoA-II mixed discoidal HDL particles (11).

Acknowledgments—We thank Dr. Phillip Howles for valuable discussions. We also thank Cali Smith for excellent administrative assistance.

REFERENCES

1. Barter, P., Kastelein, J., Nunn, A., and Hobbs, R. (2003) High density lipoproteins (HDLs) and atherosclerosis. The unanswered questions. *Atherosclerosis* **168,** 195–211
2. Barter, P. J., Nicholls, S., Rye, K. A., Anantharamaiah, G. M., Navab, M., and Fogelman, A. M. (2004) Anti-inflammatory properties of HDL. *Circ. Res.* **95,** 764–772
3. Rader, D. J. (2002) High density lipoproteins and atherosclerosis. *Am. J. Cardiol.* **90,** 62i-70i
4. Asztalos, B. F. (2004) High density lipoprotein metabolism and progression of atherosclerosis. New insights from the HDL Atherosclerosis Treatment Study. *Curr. Opin. Cardiol.* **19,** 385–391
5. Grunfeld, C., and Feingold, K. R. (2008) HDL and innate immunity. A tale of two apolipoproteins. *J. Lipid Res.* **49,** 1605–1606
6. Nielsen, M. J., Nielsen, L. B., and Moestrup, S. K. (2006) High density lipoproteins and innate immunity. *Future Lipidol.* **1,** 729–734
7. Nofer, J. R., Brodde, M. F., and Kehrel, B. E. (2010) High density lipoproteins, platelets, and the pathogenesis of atherosclerosis. *Clin. Exp. Pharmacol. Physiol.* **37,** 726–735
8. Davidson, W. S., Silva, R. A., Chantepie, S., Lagor, W. R., Chapman, M. J., and Kontush, A. (2009) Proteomic analysis of defined HDL subpopulations reveals particle-specific protein clusters. Relevance to antioxidative function. *Arterioscler. Thromb. Vasc. Biol.* **29,** 870–876
9. Vaisar, T., Pennathur, S., Green, P. S., Gharib, S. A., Hoofnagle, A. N., Cheung, M. C., Byun, J., Vuletic, S., Kassim, S., Singh, P., Chea, H., Knopp, R. H., Brunzell, J., Geary, R., Chait, A., Zhao, X. Q., Elkon, K., Marcovina, S., Ridker, P., Oram, J. F., and Heinecke, J. W. (2007) Shotgun proteomics implicates protease inhibition and complement activation in the anti-inflammatory properties of HDL. *J. Clin. Invest.* **117,** 746–756
10. Havel, P. J., Goldstein, J. L., and Brown, M. S. (1980) in *The Metabolic Control of Disease* (Bondy, P. K., and Rosenburg, L. E., eds) pp. 393–494, W. B. Saunder Co., Philadelphia, PA
11. Durbin, D. M., and Jonas, A. (1997) The effect of apolipoprotein A-II on the structure and function of apolipoprotein A-I in a homogeneous reconstituted high density lipoprotein particle. *J. Biol. Chem.* **272,** 31333–31339
12. Gauthamadasa, K., Rosales, C., Pownall, H. J., Macha, S., Jerome, W. G., Huang, R., and Silva, R. A. (2010) Speciated human high density lipoprotein protein proximity profiles. *Biochemistry* **49,** 10656–10665
13. Huang, R., Silva, R. A., Jerome, W. G., Kontush, A., Chapman, M. J., Curtiss, L. K., Hodges, T. J., and Davidson, W. S. (2011) Apolipoprotein A-I structural organization in high density lipoproteins isolated from human plasma. *Nat. Struct. Mol. Biol.* **18,** 416–422
14. Rosales, C., Gillard, B. K., Courtney, H. S., Blanco-Vaca, F., and Pownall, H. J. (2009) Apolipoprotein modulation of streptococcal serum opacity factor activity against human plasma high density lipoproteins. *Biochemistry* **48,** 8070–8076
15. Birjmohun, R. S., Dallinga-Thie, G. M., Kuivenhoven, J. A., Stroes, E. S., Otvos, J. D., Wareham, N. J., Luben, R., Kastelein, J. J., Khaw, K. T., and Boekholdt, S. M. (2007) Apolipoprotein A-II is inversely associated with risk of future coronary artery disease. *Circulation* **116,** 2029–2035
16. Buring, J. E., O'Connor, G. T., Goldhaber, S. Z., Rosner, B., Herbert, P. N., Blum, C. B., Breslow, J. L., and Hennekens, C. H. (1992) Decreased HDL2 and HDL3 cholesterol, apoA-I and apoA-II, and increased risk of myocardial infarction. *Circulation* **85,** 22–29
17. Roselli della Rovere, G., Lapolla, A., Sartore, G., Rossetti, C., Zambon, S., Minicuci, N., Crepaldi, G., Fedele, D., and Manzato, E. (2003) Plasma lipoproteins, apoproteins and cardiovascular disease in type 2 diabetic patients. A nine-year follow-up study. *Nutr. Metab. Cardiovasc. Dis.* **13,** 46–51
18. Tailleux, A., Duriez, P., Fruchart, J. C., and Clavey, V. (2002) Apolipoprotein A-II, HDL metabolism, and atherosclerosis. *Atherosclerosis* **164,** 1–13
19. Broedl, U. C., Jin, W., Fuki, I. V., Millar, J. S., and Rader, D. J. (2006)

Endothelial lipase is less effective at influencing HDL metabolism *in vivo* in mice expressing apoA-II. *J. Lipid Res.* **47,** 2191–2197
20. Castellani, L. W., Nguyen, C. N., Charugundla, S., Weinstein, M. M., Doan, C. X., Blaner, W. S., Wongsiriroj, N., and Lusis, A. J. (2008) Apolipoprotein AII is a regulator of very low density lipoprotein metabolism and insulin resistance. *J. Biol. Chem.* **283,** 11633–11644
21. de Beer, M. C., Durbin, D. M., Cai, L., Mirocha, N., Jonas, A., Webb, N. R., de Beer, F. C., and van Der Westhuyzen, D. R. (2001) Apolipoprotein A-II modulates the binding and selective lipid uptake of reconstituted high density lipoprotein by scavenger receptor BI. *J. Biol. Chem.* **276,** 15832–15839
22. Jonas, A. (2002) in *Biochemistry of Lipids, Lipoproteins and Membranes* (Vance, D. E., and Vance, J. E., eds) pp. 483–504, Elsevier Science, Amsterdam
23. Boucher, J., Ramsamy, T. A., Braschi, S., Sahoo, D., Neville, T. A., and Sparks, D. L. (2004) Apolipoprotein A-II regulates HDL stability and affects hepatic lipase association and activity. *J. Lipid Res.* **45,** 849–858
24. Rye, K. A., Wee, K., Curtiss, L. K., Bonnet, D. J., and Barter, P. J. (2003) Apolipoprotein A-II inhibits high density lipoprotein remodeling and lipid-poor apolipoprotein A-I formation. *J. Biol. Chem.* **278,** 22530–22536
25. Lund-Katz, S., and Phillips, M. C. (1986) Packing of cholesterol molecules in human low density lipoprotein. *Biochemistry* **25,** 1562–1568
26. Silva, R. A., Hilliard, G. M., Li, L., Segrest, J. P., and Davidson, W. S. (2005) A mass spectrometric determination of the conformation of dimeric apolipoprotein A-I in discoidal high density lipoproteins. *Biochemistry* **44,** 8600–8607
27. Maiorano, J. N., Jandacek, R. J., Horace, E. M., and Davidson, W. S. (2004) Identification and structural ramifications of a hinge domain in apolipoprotein A-I discoidal high density lipoproteins of different size. *Biochemistry* **43,** 11717–11726
28. Markwell, M. A., Haas, S. M., Bieber, L. L., and Tolbert, N. E. (1978) A modification of the Lowry procedure to simplify protein determination in membrane and lipoprotein samples. *Anal. Biochem.* **87,** 206–210
29. Massey, J. B., Pownall, H. J., Macha, S., Morris, J., Tubb, M. R., and Silva, R. A. (2009) Mass spectrometric determination of apolipoprotein molecular stoichiometry in reconstituted high density lipoprotein particles. *J. Lipid Res.* **50,** 1229–1236
30. Zhang, Z., and Smith, D. L. (1993) Determination of amide hydrogen exchange by mass spectrometry. A new tool for protein structure elucidation. *Protein Sci.* **2,** 522–531
31. Wu, Z., Wagner, M. A., Zheng, L., Parks, J. S., Shy, J. M., 3rd, Smith, J. D., Gogonea, V., and Hazen, S. L. (2007) The refined structure of nascent HDL reveals a key functional domain for particle maturation and dysfunction. *Nat. Struct. Mol. Biol.* **14,** 861–868
32. Chetty, P. S., Mayne, L., Lund-Katz, S., Stranz, D., Englander, S. W., and Phillips, M. C. (2009) Helical structure and stability in human apolipoprotein A-I by hydrogen exchange and mass spectrometry. *Proc. Natl. Acad. Sci. U.S.A.* **106,** 19005–19010
33. Matz, C. E., and Jonas, A. (1982) Reaction of human lecithin:cholesterol acyltransferase with synthetic micellar complexes of apolipoprotein A-I, phosphatidylcholine, and cholesterol. *J. Biol. Chem.* **257,** 4541–4546
34. Silva, R. A., Schneeweis, L. A., Krishnan, S. C., Zhang, X., Axelsen, P. H., and Davidson, W. S. (2007) The structure of apolipoprotein A-II in discoidal high density lipoproteins. *J. Biol. Chem.* **282,** 9713–9721
35. Silva, R. A., Huang, R., Morris, J., Fang, J., Gracheva, E. O., Ren, G., Kontush, A., Jerome, W. G., Rye, K. A., and Davidson, W. S. (2008) Structure of apolipoprotein A-I in spherical high density lipoproteins of different sizes. *Proc. Natl. Acad. Sci. U.S.A.* **105,** 12176–12181
36. Bhat, S., Sorci-Thomas, M. G., Alexander, E. T., Samuel, M. P., and Thomas, M. J. (2005) Intermolecular contact between globular N-terminal fold and C-terminal domain of apoA-I stabilizes its lipid-bound conformation. Studies employing chemical cross-linking and mass spectrometry. *J. Biol. Chem.* **280,** 33015–33025
37. Martin, D. D., Budamagunta, M. S., Ryan, R. O., Voss, J. C., and Oda, M. N. (2006) Apolipoprotein A-I assumes a "looped belt" conformation on reconstituted high density lipoprotein. *J. Biol. Chem.* **281,** 20418–20426
38. Lou, X., van Dongen, J. L., Vekemans, J. A., and Meijer, E. W. (2009) Matrix suppression and analyte suppression effects of quaternary ammonium salts in matrix-assisted laser desorption/ionization time-of-flight mass spectrometry. An investigation of suppression mechanism. *Rapid Commun. Mass Spectrom.* **23,** 3077–3082
39. Annesley, T. M. (2003) Ion suppression in mass spectrometry. *Clin. Chem.* **49,** 1041–1044
40. Glocker, M. O., Borchers, C., Fiedler, W., Suckau, D., and Przybylski, M. (1994) Molecular characterization of surface topology in protein tertiary structures by aminoacylation and mass spectrometric peptide mapping. *Bioconjug. Chem.* **5,** 583–590
41. Zappacosta, F., Ingallinella, P., Scaloni, A., Pessi, A., Bianchi, E., Sollazzo, M., Tramontano, A., Marino, G., and Pucci, P. (1997) Surface topology of Minibody by selective chemical modifications and mass spectrometry. *Protein Sci.* **6,** 1901–1909
42. Ohguro, H., Palczewski, K., Walsh, K. A., and Johnson, R. S. (1994) Topographic study of arrestin using differential chemical modifications and hydrogen/deuterium exchange. *Protein Sci.* **3,** 2428–2434
43. Ji, Y., and Jonas, A. (1995) Properties of an N-terminal proteolytic fragment of apolipoprotein A-I in solution and in reconstituted high density lipoproteins. *J. Biol. Chem.* **270,** 11290–11297
44. Panagotopulos, S. E., Horace, E. M., Maiorano, J. N., and Davidson, W. S. (2001) Apolipoprotein A-I adopts a belt-like orientation in reconstituted high density lipoproteins. *J. Biol. Chem.* **276,** 42965–42970
45. Davidson, W. S., and Hilliard, G. M. (2003) The spatial organization of apolipoprotein A-I on the edge of discoidal high density lipoprotein particles. A mass specrometry study. *J. Biol. Chem.* **278,** 27199–27207
46. Wu, Z., Gogonea, V., Lee, X., Wagner, M. A., Li, X. M., Huang, Y., Undurti, A., May, R. P., Haertlein, M., Moulin, M., Gutsche, I., Zaccai, G., Didonato, J. A., and Hazen, S. L. (2009) Double superhelix model of high density lipoprotein. *J. Biol. Chem.* **284,** 36605–36619
47. Koppaka, V., Silvestro, L., Engler, J. A., Brouillette, C. G., and Axelsen, P. H. (1999) The structure of human lipoprotein A-I. Evidence for the "belt" model. *J. Biol. Chem.* **274,** 14541–14544
48. Segrest, J. P., Jones, M. K., Klon, A. E., Sheldahl, C. J., Hellinger, M., De Loof, H., and Harvey, S. C. (1999) A detailed molecular belt model for apolipoprotein A-I in discoidal high density lipoprotein. *J. Biol. Chem.* **274,** 31755–31758
49. Catte, A., Patterson, J. C., Jones, M. K., Jerome, W. G., Bashtovyy, D., Su, Z., Gu, F., Chen, J., Aliste, M. P., Harvey, S. C., Li, L., Weinstein, G., and Segrest, J. P. (2006) Novel changes in discoidal high density lipoprotein morphology. A molecular dynamics study. *Biophys. J.* **90,** 4345–4360
50. Sorci-Thomas, M., Kearns, M. W., and Lee, J. P. (1993) Apolipoprotein A-I domains involved in lecithin-cholesterol acyltransferase activation. Structure:function relationships. *J. Biol. Chem.* **268,** 21403–21409
51. Sviridov, D., Hoang, A., Sawyer, W. H., and Fidge, N. H. (2000) Identification of a sequence of apolipoprotein A-I associated with the activation of lecithin:cholesterol acyltransferase. *J. Biol. Chem.* **275,** 19707–19712